Phosphatidylserine Membrane Domain Clustering Induced by Annexin A2/S100A10 Heterotetramer†

Manuela Menke,‡ Volker Gerke,§ and Claudia Steinem*,‡

Institut für Analytische Chemie, Chemo- und Biosensorik, Universität Regensburg, 93040 Regensburg, Germany, and Institut für Medizinische Biochemie, Zentrum für Molekularbiologie der Entzündung, Westfälische Wilhelms-Universität, von-Esmarch-Str. 56, 48149 Münster, Germany

Received August 10, 2005

ABSTRACT: By means of scanning force and fluorescence microscopy of artificial membranes immobilized on mica surfaces, the lateral organization of the annexin A2/S100A10 heterotetramer (annexin A2t) and its influence on the lateral organization of the lipids within the membrane have been elucidated. Planar lipid bilayers composed of 1-palmitoyl-2-oleoyl-*sn*-glycero-3-phosphocholine (POPC)/1-palmitoyl-2-oleoyl-*sn*-glycero-3-phosphoserine (POPS) were prepared on atomically flat mica surfaces by the spreading of unilamellar vesicles. Fluorescence images of fluorescently labeled annexin A2t and scanning force microscopy images of nonlabeled protein bound to POPC/POPS bilayers show the formation of micrometer-sized lateral protein domains in the presence of 1 mM $CaCl_2$. By means of scanning force microscopy, not only protein domains became discernible but also small membrane domains, which were attributed to POPS-enriched areas. A depletion of these POPS domains was observed in the vicinity of annexin A2t protein domains. These results indicate that annexin A2t is a peripheral membrane-binding complex capable of inducing lipid segregation.

Annexin A2 is a member of the annexin protein family, which is defined by the unique structural and biochemical features of its members (reviewed in refs *1*−*3*). Because of their characteristic Ca^{2+}-dependent membrane binding, annexins have been implicated in several membrane-related events such as endo- and exocytosis and membrane−cytoskeleton interactions. The conserved Ca^{2+}- and membrane-binding module is the annexin core consisting of four repeats, each of which is composed of five α helices (for a review, see ref *4*). In each annexin, the core is preceded by a N-terminal domain that varies in length and sequence and can mediate interactions with protein ligands and regulate the annexin−membrane association.

In cells, annexin A2 is found as a monomer (A2m) and as a heterotetramer (A2t) consisting of two annexin A2 molecules and one S100A10 (p11) dimer, which is a member of the Ca^{2+}-binding S100-protein family (*5*). Annexin A2t is mainly localized at endosomes and the plasma membrane (*6*−*9*), while the monomer is mainly cytosolic.

Even though the role of annexin A2t is still not fully understood, recent RNA interference experiments have disclosed several cellular processes by the downregulation of annexin A2. The transient knockdown produced defects in the generation of multivesicular endosomal carrier vesicles on early endosomes, in the morphology and distribution of recycling endosomes and certain Ca^{2+}-regulated exocytosis events (*9*−*12*). The results implicate that annexin A2 has a scaffolding and structural function on certain cellular membranes such as endosomal membranes. Sites of actin assembly at cellular membranes have also been identified in different cell types at points to which annexin A2 is specifically recruited. For example, membrane microdomain organization in smooth muscle cells, which is stabilized by interactions with an underlying actin cytoskeleton, appears to be regulated by annexin A2 (*13*), and the protein is recruited to actin-rich membrane areas characterized by a high cholesterol and phosphatidylinositol-(4,5)-bisphosphate content (*3*, *14*−*17*). Cholesterol depletion or sequestration precludes this interaction of annexin A2 and influences the specific actin assembly, indicating that membrane-bound annexin A2 serves as a platform for actin assembly (for a review, see ref *17*). Chasserot-Golaz et al. (*9*) recently found that the reduction of annexin A2 at the cell periphery strongly inhibits exocytosis. It was shown that annexin A2t is capable of promoting the formation of G_{M1}-containing lipid microdomains required for calcium-regulated exocytosis. They propose that annexin A2 acts as a calcium-dependent promoter of lipid microdomains required for structural and spatial organization of the exocytotic machinery.

On the basis of our own findings (*18*) and those described above, it is proposed that annexin A2t bound to a lipid membrane forms two-dimensional protein clusters and recruits certain lipid components underneath these clusters. This establishes and stabilizes a protein platform capable of recruiting other (cytosolic and cytoskeletal) components and of structuring lipids within the plane of the membrane. To prove this hypothesis, we performed fluorescence and

† This work was supported by the DFG graduate college 760.

* To whom correspondence should be addressed. Telephone: +49-941-943-4548. Fax: +49-941-943-4491. E-mail: claudia.steinem@chemie.uni-regensburg.de.

‡ Universität Regensburg.

§ Westfälische Wilhelms-Universität.

10.1021/bi051585i CCC: $30.25
Published on Web 10/29/2005

scanning force microscopy (SFM)[1] of fluid lipid bilayers composed of 1-palmitoyl-2-oleoyl-*sn*-glycero-3-phosphocholine (POPC) and 1-palmitoyl-2-oleoyl-*sn*-glycero-3-phosphoserine (POPS) immobilized on mica surfaces to which annexin A2t had been bound. SFM in aqueous solution enabled us to directly visualize membrane-bound annexin A2t in a highly resolved manner, thereby revealing directly the formation of protein and POPS-rich domains.

MATERIALS AND METHODS

Materials. POPC and POPS were purchased from Avanti Polar Lipids (Alabaster, AL). Heterotetrameric annexin A2t was purified from porcine intestinal endothelium according to the procedure described by Gerke and Weber (*19*). The protein concentration was determined by UV spectra using an extinction coefficient of $\epsilon_{280\ nm} = 0.65\ cm^2\ mg^{-1}$. TEXAS RED-X Protein Labeling Kit was purchased from Molecular Probes (Eugene, OR). Silicon cantilevers were purchased from Ultrasharp (CSC 37/50 E, Silicon-MDT Ltd., Moscow, Russia).

Lipid Bilayer Preparation. Solid-supported lipid bilayers were prepared on mica surfaces using the vesicle-spreading technique. First, POPC and POPS each dissolved in chloroform were mixed in a molar ratio of 4:1, dried at the bottom of glass test tubes by a stream of nitrogen, and desiccated under vacuum for 3 h, resulting in lipid films covering the bottom of the glass test tubes. The lipid films were rehydrated by the addition of buffer composed of 20 mM TRIS/HCl, 100 mM NaCl, and 1 mM NaN_3 at pH 7.4, leading to a final lipid concentration of 1 mg/mL, and vortexed several times. The resulting multilamellar vesicles were converted into unilamellar ones by the extrusion method using a LiposoFast extruder (Avestin, Inc., Ottawa, Canada) supplied with a 50 nm polycarbonate membrane. Freshly cleaved mica was covered with the unilamellar vesicle suspension (0.5 mg/mL), and Ca^{2+} ions were added up to a final concentration of 10 mM from a 1 M $CaCl_2$ stock solution. After 1 h at room temperature, the mica surface was rinsed with buffer solution (20 mM TRIS/HCl, 100 mM NaCl, 1 mM $CaCl_2$, and 1 mM NaN_3 at pH 7.4).

Fluorescence Microscopy. Protein labeling was performed using TEXAS RED-X following the instructions of the manufacturer. Briefly, 1 mg of annexin A2t was reacted with one vial of TEXAS RED-X carrying a succinimidyl ester moiety, which efficiently reacts with primary amines of the protein to form stable dye−protein conjugates. A dye/protein ratio of 1:1 was obtained. Fluorescence images were obtained with an Axiotech Vario microscope (Carl Zeiss, Göttingen, Germany) equipped with an Achroplan 40×/0.80 W objective. Filter set 45 (BP 560/40, FT 585, BP 630/75) was used for fluorescence light detection. A stock solution of labeled annexin A2t was added to a POPC/POPS lipid bilayer attached to a mica surface with a minimum final concentration of 0.3 μM to ensure maximal protein binding (*18*). After 15 min of incubation, the surface was rinsed several times with buffer to remove nonbound protein from the solution. All measurements were carried out in aqueous buffer solution (20 mM TRIS/HCl, 100 mM NaCl, 1 mM $CaCl_2$, and 1 mM NaN_3 at pH 7.4).

SFM. SFM of lipid bilayers was performed using a JPK NanoWizard scanning force microscope (JPK Instruments, Berlin, Germany). A stock solution of nonlabeled protein was added to a POPC/POPS lipid bilayer attached to a mica surface with a minimum final concentration of 0.3 μM, and after a 15 min incubation period, the surface was rinsed several times with buffer to remove non- and reversibly bound protein from solution. SFM images were obtained in contact or intermittent contact mode in 20 mM TRIS/HCl, 100 mM NaCl, 1 mM $CaCl_2$, and 1 mM NaN_3 at pH 7.4 using an open Teflon fluid chamber. Silicon cantilevers with a typical resonant frequency of 21 kHz and a nominal spring constant of 0.3 N m^{-1} were used. Scan rates were set to 0.3 Hz. Image resolution was 512 × 512 pixels.

RESULTS

Several studies suggest that the hetereotetrameric complex annexin A2t forms lateral protein clusters when bound to the membrane and is involved in membrane organization processes (for a review, see ref *20*). To address these questions, we investigated the lateral distribution of annexin A2t bound to phospholipid membranes. Solid-supported membranes composed of POPC and POPS were used as a simple mimic for the inner leaflet of a biological membrane. This lipid system has been shown to be well-suited to investigate annexin−membrane interactions (*18*, *21*). By means of the vesicle-spreading technique starting from unilamellar vesicles with a nominal diameter of 50 nm, POPC/POPS bilayers were successfully prepared on freshly cleaved mica surfaces in the presence of Ca^{2+} ions.

Fluorescence Images. To first visualize the organization of membrane-bound annexin A2t by fluorescence microscopy, the protein was fluorescently labeled. The ability of fluorescently labeled annexin A2t to bind to phospholipids in a manner identical to that of the nonmodified protein was proven by Ca^{2+}-dependent liposome-pelleting assays using POPC/POPS vesicles (not shown). The protein was added to POPC/POPS membranes immobilized on mica surfaces in the presence of 1 mM $CaCl_2$ for 15 min. Prior to the addition of fluorescently labeled annexin A2t, the mica surface with the attached POPC/POPS bilayer appears almost black (Figure 1A) under the fluorescence microscope in aqueous solution. After the protein was added and rinsed with a 1 mM $CaCl_2$-containing buffer to remove nonbound protein from solution, fluorescence images were taken, which show a nonhomogeneous distribution of bright spots with different sizes on the membrane surface, indicating that annexin A2t has been bound on the membrane in an irreversible manner (parts B and C of Figure 1). The total surface coverage of irreversibly bound protein was determined to be 11 ± 4% (n = 13) by pixel analysis. As a control, fluorescently labeled annexin A2t was added to a POPC/POPS membrane in the absence of $CaCl_2$. No bright spots were observed, confirming that the annexin A2t−membrane interaction is strictly calcium-ion-dependent (not shown). The bright spots observed in the presence of Ca^{2+} clearly show that lateral protein clustering on the membrane

[1] Abbreviations: DOPC, 1,2-dioleoyl-*sn*-glycero-3-phosphocholine; DOPS, 1,2-dioleoyl-*sn*-glycero-3-phosphoserine; EGTA, ethylene glycol bis(β-aminoethyl ether)-*N*,*N*,*N*′*N*′-tetraacetic acid; PC, phosphatidylcholine; PG, phosphatidylglycerol; POPC, 1-palmitoyl-2-oleoyl-*sn*-glycero-3-phosphocholine; POPS, 1-palmitoyl-2-oleoyl-*sn*-glycero-3-phosphoserine; PS, phosphatidylserine; SFM, scanning force microscopy.

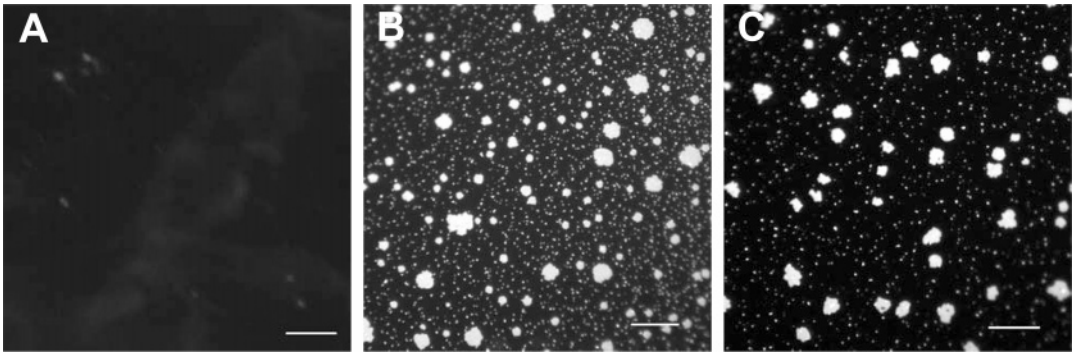

FIGURE 1: (A) Fluorescence image of a POPC/POPS (4:1) lipid bilayer deposited onto a mica surface by vesicle spreading. (B and C) Characteristic fluorescence images after the addition of 0.3 μM fluorescently labeled annexin A2t. Images were taken in buffer solution (20 mM TRIS/HCl, 100 mM NaCl, 1 mM $CaCl_2$, and 1 mM NaN_3 at pH 7.4). Scale bar length = 20 μm.

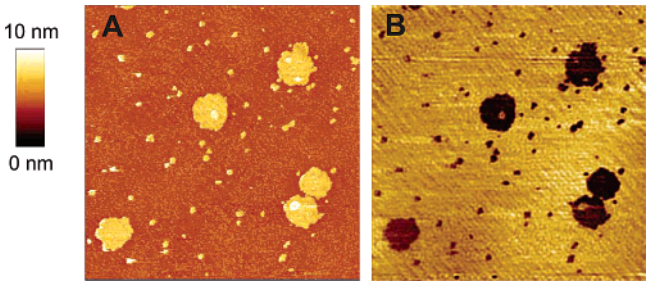

FIGURE 2: (A) SFM image (topography) of a POPC/POPS (4:1) lipid bilayer immobilized on a mica surface after the addition of 0.3 μM annexin A2t. (B) Lateral force microscopy image of the same area. The darker areas are assigned to protein domains that differ from the membrane in their material properties. Images were taken in buffer solution (20 mM TRIS/HCl, 100 mM NaCl, 1 mM $CaCl_2$, and 1 mM NaN_3 at pH 7.4). Image sizes = 40 × 40 μm^2.

surface occurs and that the protein does not bind homogeneously on the surface.

SFM Images. To obtain a higher resolution of the observed protein domains, SFM images were taken. This technique bears the advantage that artifacts arising from labeling of the protein can be excluded and that topographic features of the protein layer can be obtained. Annexin A2t was again added to a mica-attached POPC/POPS membrane in the presence of 1 mM $CaCl_2$. After the nonbound protein was removed, SFM images were taken in aqueous solution. A typical topographic image is depicted in Figure 2A. Protein domains similar to those observed by fluorescence microscopy are visible as brighter areas. The height distribution of the protein domains is very even except for some higher spots, indicating that the protein binds in a defined manner to the lipid bilayer. The higher structures are located mostly at the rim of a protein domain or as a round cluster on top and have about twice the height of a single protein layer, thus, indicative of the assembly of a second annexin layer. Also, the domain distribution resembles that found by fluorescence microscopy.

To corroborate that the protein-dependent structures can be assigned to a material that is different from the lipid bilayer, i.e., membrane-bound annexin A2t, we performed lateral force microscopy. In lateral force microscopy images, the observed contrast is a result of differences in the torsion of the cantilever caused by different friction forces acting on the cantilever. In Figure 2B, a backward scan is shown, in which the darker areas indicate larger friction than on the brighter ones. Lateral force microscopy has been shown to be a useful tool to visualize material contrasts (*22*) and

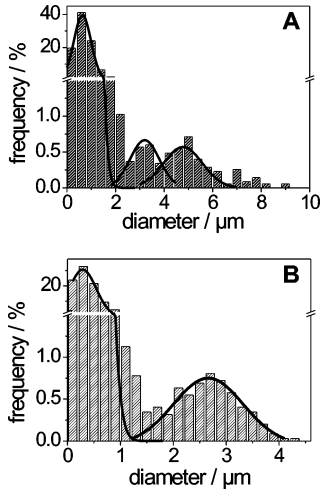

FIGURE 3: (A) Size distribution of annexin A2t clusters obtained by brightness-based pixel analysis from fluorescent images. Three Gaussian distributions were fit to the data shown as solid lines. (B) Size distribution of annexin A2t protein domains obtained from SFM images indicating two distinct protein domain populations. The solid lines represent Gaussian fits to the data.

demonstrates here that a different material, which is a membrane-bound protein, has been adsorbed to the lipid bilayer.

Protein Domain Size. Fluorescence as well as SFM images suggest that there are at least two different protein domain sizes visible on the bilayer. To investigate this in more detail, the size distribution of the protein domains was determined by pixel analysis. For fluorescence images, binning was set to 400 nm because of the microscope resolution, while for SFM images, the binning was set to 200 nm (parts A and B of Figure 3). A total of 95% of the detected protein domains are smaller than 2 μm in diameter. Even though the number of small domains is much larger than that of domains, which are larger than 2 μm, about 64% of the protein is bound in domains larger than 2 μm in diameter. The size distribution of the protein domains obtained from fluorescence images by pixel analysis is depicted in Figure 3A. Three different domain populations differing in their mean diameters are discernible. Most domains are found to be in the range of 600 ± 300 nm, while part of them are 3.2 ± 0.6 and 4.8 ± 0.8 μm in diameter. The domain distribution obtained from SFM images is very similar, even though only a few lateral protein aggregates with a diameter larger than 4 μm are found in the SFM images (Figure 3B). The larger protein domains also show a Gaussian-like distribution with a mean diameter

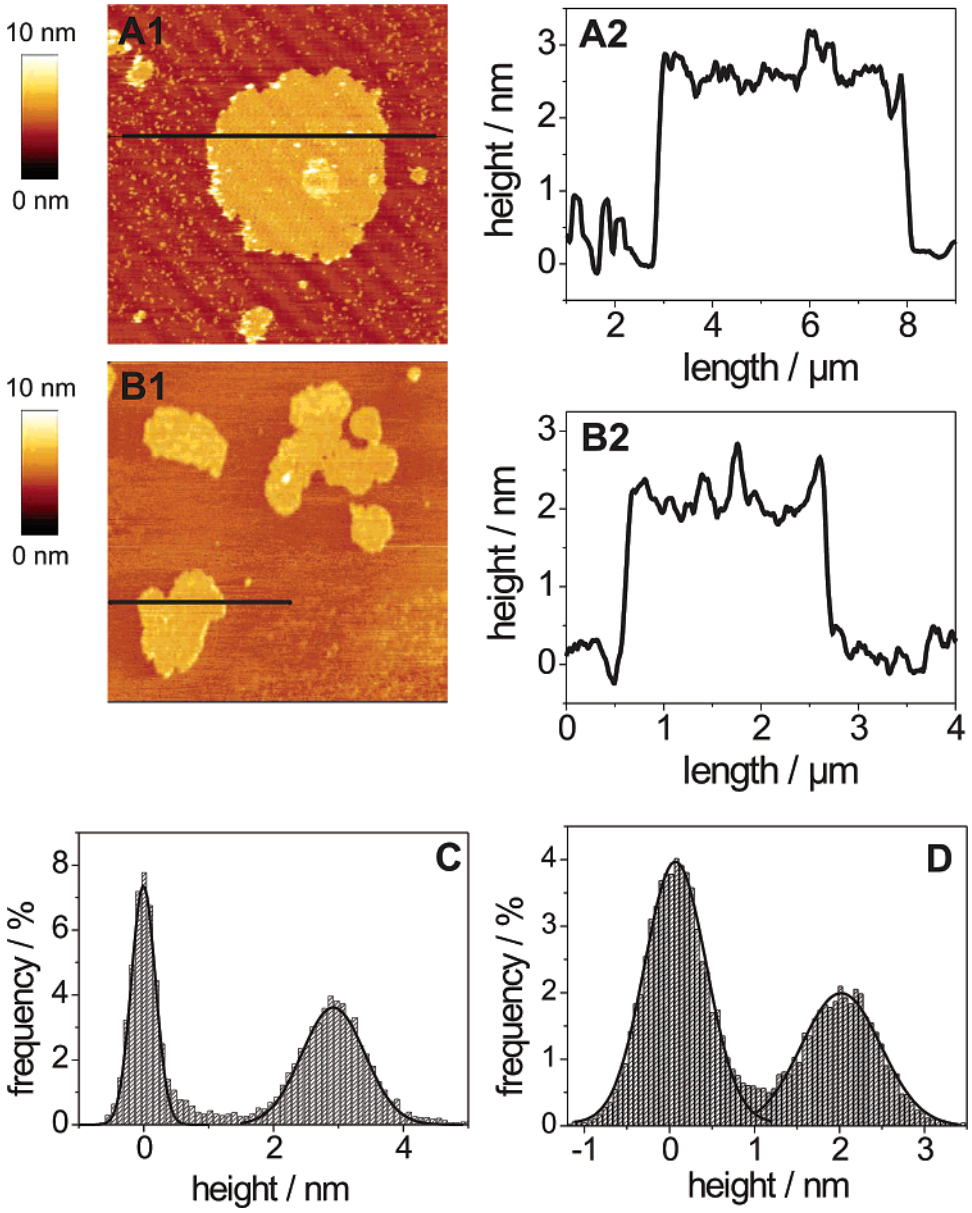

FIGURE 4: Topographic images of protein domains obtained in (A1) contact and (B1) intermittent contact mode. The corresponding line scans (A2 and B2) are depicted on the right-hand side. For contact mode, the observed height difference between the lipid bilayer and the protein layer is about 2.6 nm, while for intermittent contact, the cross-section indicates a protein height of approximately 2 nm. Histogram analysis for contact and intermittent contact mode revealed an average height of 2.6 ± 0.4 nm (n = 17) and 2.0 ± 0.2 nm (n = 23), respectively. Typical height analysis histogram of a protein domain obtained in contact mode (C) and intermittent contact mode (D). The two well-separated peaks are attributed to the lipid surface (set to 0) and the protein layer. Images were obtained in aqueous solution (20 mM TRIS/HCl, 100 mM NaCl, 1 mM $CaCl_2$, and 1 mM NaN_3 at pH 7.4). Image size = (A1) 10 × 10 μm^2 and (B1) 8 × 8 μm^2.

of 2.6 ± 0.7 μm, while most of the domains are in the range of 300 ± 100 nm.

Protein Domain Height. The height of the protein domains was investigated by line scans. Dependent upon whether the images were taken in contact or intermittent contact mode, slightly different protein domain heights were obtained. In contact mode, a typical height difference between the protein domain and the lipid bilayer of about 2.6 nm was measured (Figure 4A), while the height extracted from intermittent contact mode was in the range of 2.0 nm (Figure 4B). A more detailed histogram analysis of several protein domains leads to an average height of 2.6 ± 0.4 nm (n = 17) for contact mode images (Figure 4C) and 2.0 ± 0.2 nm (n = 23) for intermittent contact mode images (Figure 4D). The higher structures found on top of some domains show a height of about 3−4 nm in contact mode, indicating a second protein layer.

Lipid Membrane Structure. Besides the large protein domains, a fine structure was also visible in the SFM images that was not seen by fluorescence microscopy. We propose that this fine structure is a result of small phosphatidylserine (PS) membrane domains. The question arose whether these membrane domains are induced by annexin A2t or whether they are already present prior the addition of the protein. To answer this question, we investigated POPC/POPS membranes in the presence of 1 mM $CaCl_2$ in the absence of protein. Figure 5 shows topographic images of a POPC/POPS lipid bilayer obtained in a 1 mM $CaCl_2$-containing buffer. Higher domain structures are clearly visible, which we assign to small phase-separated PS domains. These domains are

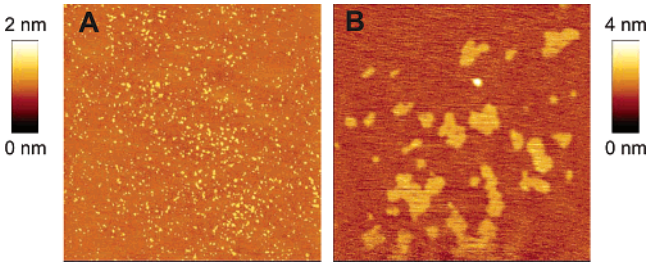

FIGURE 5: (A) SFM image of a POPC/POPS (4:1) lipid bilayer prepared by vesicle spreading onto a mica surface. (B) Magnification of POPS-enriched microdomains. The height difference of these structures depends upon the applied force and was determined to be between 0.4 and 1 nm. Image sizes = (A) 10 × 10 μm^2 and (B) 550 × 550 nm^2.

present in POPC/POPS lipid bilayers in the presence of 1 mM $CaCl_2$ without the addition of protein. They are very irregularly shaped, with mean diameters of about 20−100 nm, and are more or less homogeneously distributed in the membrane. The percentage of area occupied with POPS microdomains varied among the preparations and was found to be between 5 and 15%. The height difference between those domains and the surrounding matrix is 0.4−1 nm dependent upon the applied force. This finding suggests that the higher areas are probably more rigid and thus less easily indented by the SFM tip than the surrounding area. This idea is corroborated by the observation that Ca^{2+} removal by rinsing with an ethylene glycol bis(*β*-aminoethyl ether)-*N*,*N*,*N*′*N*′-tetraacetic acid (EGTA)-containing buffer results in a disappearance of these membrane domains, leaving a flat and featureless membrane surface behind (data not shown).

Depletion of POPS Domains. The most interesting observation of our study is that the POPS microdomains appear to be less frequent in the vicinity of the annexin A2t protein domains than in areas where no protein is bound. Figure 6A shows a deflection image to illustrate this observation. To quantify the inhomogeneity of the POPS domain distribution, we divided the entire area in equidistant rings and determined the area of POPS microdomains per ring area by pixel analysis. A typical example of this procedure is given in Figure 6B. In the topography image, the equidistant rings drawn around a protein domain are shown as black lines. The region between two lines corresponds to the ring area. In each ring area, the part that is covered by POPS molecules observed as brighter domains is determined. In Figure 6C, the fraction of POPS-covered area per ring area is plotted versus the distance from the protein domain. The edge of the protein domain is set to 0. The plot clearly shows that there is a depletion of POPS domains close to the protein domain. To ensure that this depletion is a result of the protein domain, the POPS distribution was also determined in regions without a protein domain in close proximity and on membranes without adsorbed proteins. One characteristic result is plotted in Figure 6C. An equal distribution of POPS domains is found independent of the distance from a certain but arbitrarily defined starting point. At a certain distance from the protein domain, the coverage with POPS domains is the same as that observed at any other area further away from the protein domains.

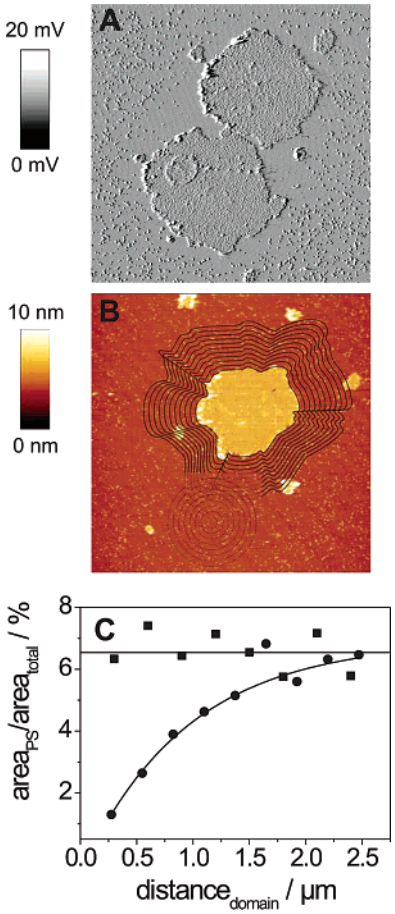

FIGURE 6: (A) Vertical deflection SFM image of two annexin A2t protein domains on a POPC/POPS lipid bilayer on mica. (B) Topographic image of an annexin A2t protein domain. The black rings indicate the ring areas used for the analysis shown on the right-hand side. (C) Area of lipid domains enriched in negatively charged POPS molecules per ring area plotted versus the distance from the protein aggregate (●) and an arbitrarily used spot far away from a protein domain (■). Image sizes = (A) 11.2 × 11.2 μm^2 and (B) 15 × 15 μm^2.

DISCUSSION

The central biochemical characteristic of all annexins including annexin A2t is their Ca^{2+}-regulated binding to membranes containing acidic phospholipids. The specific protein−lipid interaction in combination with protein−protein interactions might enable them to reorganize the cytoplasmic leaflet of cellular membranes, thus forming a structural prerequisite for certain membrane-trafficking events and providing a platform for cytoskeleton organization (e.g., actin assembly) (for a review, see ref *20*). In the case of annexin A2t, this platform is discussed in terms of lateral aggregates of annexin A2t (*3*). Several results have suggested that annexin A2t is a regulating element in membrane dynamics and the organization especially of cholesterol and sphingomyelin-enriched microdomains (*13*, *15*). A number of studies demonstrated a nonuniform distribution of annexin A2 on cellular membranes and an annexin A2-mediated reorganization of lipid rafts and the underlying actin cytoskeleton (*2*, *14*, *23*).

Our study presents direct evidence that annexin A2t forms two-dimensional lateral protein aggregates. Fluid lipid bilayers composed of PS and phosphatidylcholine (PC) immobilized on mica surfaces were used to mimic the inner

leaflet of the plasma membrane. Although being a very simple system, artificial membranes have been demonstrated to be a useful tool to investigate annexin−membrane interactions (*18*, *24*, *25*). Visualization of the lateral organization of annexin A2t bound to these membranes was realized by means of microscopy techniques. Fluorescence microscopy as well as SFM unambiguously showed that lateral protein aggregates are formed on the POPC/POPS lipid bilayers. What is the driving force for the formation of lateral protein aggregates? It is conceivable that specific protein−protein interactions are responsible for the formation of lateral aggregates. Large annexin A5 clusters that grow over time and crystallize in two dimensions on a membrane surface have been visualized by means of SFM (*26*−*29*). In crystal structures of annexin A5, A7 and B12 trimers have been found (*30*, *31*). The tendency to form such trimers might be attributed to specific protein−protein interactions. However, for annexin A1 and A2, no such trimer formation is reported and also no crystallization of the protein on membrane surfaces was observed (*32*). Another explanation for the formation of lateral protein aggregates without specific protein−protein interactions is given by Hinderliter et al. (*33*). They demonstrated by Monte Carlo simulations that, if a preferential protein−anionic lipid interaction is assumed, protein domains can be formed in a process mediated only by preferential protein−lipid and lipid−lipid interactions. The model also includes the lipid redistribution induced by protein binding. Lipid reorganization induced by annexin A2t was also concluded from Ca^{2+}-titration experiments performed by the quartz crystal microbalance technique (*18*).

Surprisingly, only around 11 ± 4% of the membrane was covered with annexin A2t. If, however, POPS is clustered in membrane microdomains and 20 mol % POPS is accessible for annexin A2t binding, it is expected that at least 20% of the surface is covered by annexin A2t. Typically, the protein surface coverage is supposed to be even slightly larger because the observed POPS clusters may also contain POPC molecules. Brisson and co-workers recently provided evidence for a nonhomogeneous distribution of 1,2-dioleoyl-*sn*-glycero-3-phosphoserine (DOPS) between the two leaflets in lipid bilayers obtained from vesicle spreading on mica (*34*). They attributed this difference to a surface-induced redistribution of DOPS between the two membrane leaflets induced by the mica surface (*35*). For example, in a mixture composed of 1,2-dioleoyl-*sn*-glycero-3-phosphocholine (DOPC) and DOPS in a molar ratio of 4:1, they found only 7 mol % of the DOPS accessible for prothrombin binding. If only 7% PS molecules were accessible in our POPC/POPS membranes, an estimated protein surface coverage of around 9−12% would be expected assuming that POPS is organized in clusters similar to what we have observed in the DPPC/DPPS system (*22*, *34*). The finding that the negatively charged lipid is recruited to the membrane leaflet facing the mica surface explains why there are still POPS clusters visible that are not occupied by protein. From the topographic images, it cannot be distinguished between PS domains in the upper leaflet that are exposed to the aqueous phase and those that face the mica surface.

The height of the protein clusters as determined from line scans and histogram analysis is around 2.0−2.6 nm, dependent upon the applied SFM technique. The difference between the intermittent contact and contact mode might be a result of a stronger deformation of the fluid lipid bilayer with respect to the protein layer while scanning the surface in direct contact with the SFM probe (*36*, *37*). Independent of this difference, the height of the protein layer determined by both modes is by a factor of around two smaller than that obtained for annexin A2t bound to lipids in the gel phase. In a previous study, we determined the height of annexin A2t bound to a DPPC/DPPS (4:1) bilayer to be 4.2 nm, in good agreement with crystallographic data (*38*), assuming that both annexin monomers bind to one membrane interface. The smaller height observed here might indicate that annexin A2t partly penetrates into the lipid bilayer. A partial insertion of annexin A1 has also been shown for lipid monolayers at the air−water interface (*39*). However, it cannot be ruled out that the force applied by the scanning force microscope tip might also influence the partial insertion of annexin A2t in the lipid bilayer.

SFM, which provides a high resolution of the sample surface, not only revealed the lateral organization of the annexin A2t clusters but also resolved features of the POPC/POPS lipid bilayer. Small membrane domains became discernible in the topography images, which we attribute to clusters of POPS lipids. A phase separation between PC and PS lipids mediated by Ca^{2+} ions was also observed by Ross et al. (*22*). Investigations on vesicles and lipid monolayer systems showed a Ca^{2+}-induced lateral phase separation of negatively charged PS or phosphatidic acid molecules (*40*, *41*). The height difference of the observed small domains, which are only 50−200 nm in diameter, varies dependent upon the applied force of the SFM tip and indicates that this material is stiffer than the surrounding matrix. We propose that Ca^{2+} ions bound to the PS lipids increase the rigidity of the domains. Interestingly, we were not able to observe any movement of the lipid domains within the bilayer, which might be a result of the interaction of the PS lipids via Ca^{2+} bridges with the mica surface. From the entire surface coverage with POPS domains, we conclude that not all PS molecules are organized in these domains but only a fraction, which is variable within a certain regime.

In a previous study (*18*), we have concluded from Ca^{2+}-titration experiments that different annexin A2t-binding sites exist in a POPS-containing membrane: high-affinity binding sites for annexin A2t, which are characterized by POPS clusters exhibiting a large surface charge density, and low-affinity binding sites with fewer POPS molecules involved. Once the protein is bound to the membrane, a further recruitment of PS underneath bound annexin A2t occurs, which leads to a rearrangement of the POPS molecules. If annexin A2t partially inserts or if additional membrane-spanning proteins are present in such clusters, the protein-induced organization of the membrane lipids might also affect the lipids located in the opposing leaflet of the lipid bilayer. In principle, around 20 lipids are placed underneath one annexin molecule. Our SFM images show that a depletion of negatively charged POPS in the area surrounding a protein domain occurs. This is in accordance with the notion that the annexin A2 heterotetramer is capable of clustering PS lipids in a POPC/POPS-containing lipid bilayer and thus decreases the overall number of PS molecules in its nearest neighborhood. Previous studies suggested the capacity of Ca^{2+}-dependent membrane-binding proteins to

enrich negatively charged lipids (*42*). For example, it was shown for annexin A4 that binding of the protein increases the local concentration of phosphatidylglycerol (PG) molecules in vesicles composed of PC and PG (*43*).

The recruitment of negatively charged lipids underneath a protein domain shown here *in vitro* might be the prerequisite for clustering of small membrane microdomains to larger domains *in vivo* (*3*). Annexin A2t is supposed to influence the aggregation of membrane domains (*9*, *11*). For example, if annexin A2t was bound to the plasma membrane of smooth muscle cells, the membrane fragment distribution was shifted to larger fragments (*13*). According to Lipowsky, the formation of intramembrane domains will usually lead to a difference in spontaneous curvature, and in general, the spontaneous curvature and the line tension provide a driving force for budding (*44*, *45*). Thus, a reorganization of a lipid membrane and the formation of membrane domains might also be the prerequisite for or at least support vesicle budding and/or fusion.

REFERENCES

1. Gerke, V., and Moss, S. E. (2002) Annexins: From structure to function, *Phys. Rev. 82*, 331−371.
2. Gerke, V., and Moss, S. E. (1997) Annexins and membrane dynamics, *Biochim. Biophys. Acta 1357*, 129−154.
3. Rescher, U., and Gerke, V. (2004) Annexins-unique membrane binding proteins with diverse functions, *J. Cell Sci. 117*, 2631−2639.
4. Raynal, P., and Pollard, H. B. (1994) Annexins: The problem of assessing the biological role for a gene family of multifunctional calcium- and phospholipid-binding proteins, *Biochim. Biophys. Acta 1197*, 63−93.
5. Gerke, V., and Weber, K. (1985) Calcium-dependent conformational changes in the 36-kDa subunit of intestinal protein I related to the cellular 36-kDa target of Rous sarcoma virus tyrosine kinase, *J. Biol. Chem. 260*, 1688−1695.
6. Thiel, C., Osborn, M., and Gerke, V. (1992) The tight association of the tyrosine kinase substrate annexin II with the submembranous cytoskeleton depends on intact p11- and Ca^{2+}-binding sites, *J. Cell Sci. 103*, 733−742.
7. Zokas, L., and Glenney, J. R., Jr. (1987) The calpactin light chain is tightly linked to the cytoskeletal form of calpactin I: Studies using monoclonal antibodies to calpactin subunits, *J. Cell Biol. 105*, 2111−2121.
8. Waisman, D. M. (1995) Annexin II tetramer: Structure and function, *Mol. Cell. Biochemistry 149*/*150*, 301−322.
9. Chasserot-Golaz, S., Vitale, N., Umbrecht-Jenck, E., Knight, D., Gerke, V., and Bader, M. F. (2005) Annexin 2 promotes the formation of lipid microdomains required for calcium-regulated exocytosis of dense-core vesicles, *Mol. Biol. Cell 16*, 1108−1119.
10. Mayran, N., Parton, R. G., and Gruenberg, J. (2003) Annexin II regulates multivesicular endosome biogenesis in the degradation pathway of animal cells, *EMBO J. 22*, 3242−3253.
11. Zobiack, N., Rescher, U., Laarmann, S., Michgehl, S., Schmidt, M. A., and Gerke, V. (2002) Cell-surface attachment of pedestal-forming enteropathogenic *E. coli* induces a clustering of raft components and a recruitment of annexin 2, *J. Cell Sci. 115*, 91−98.
12. Knop, M., Aareskjold, E., Bode, G., and Gerke, V. (2004) Rab3D and annexin A2 play a role in regulated secretion of vWF, but not tPA, from endothelial cells, *EMBO J. 23*, 2982−2992.
13. Babiychuk, E. B., and Draeger, A. (2000) Annexins in cell membrane dynamics. Ca^{2+}-regulated association of lipid microdomains, *J. Cell. Biol. 150*, 1113−1124.
14. Harder, T., Kellner, R., Parton, R. G., and Gruenberg, J. (1997) Specific release of membrane-bound annexin II and cortical cytoskeletal elements by sequestration of membrane cholesterol, *Mol. Biol. Cell 8*, 533−545.
15. Oliferenko, S., Paiha, K., Harder, T., Gerke, V., Schwarzler, C., Schwarz, H., Beug, H., Gunthert, U., and Huber, L. A. (1999) Analysis of CD44-containing lipid rafts: Recruitment of annexin II and stabilization by the actin cytoskeleton, *J. Cell Biol. 146*, 843−854.
16. Zobiack, N., Rescher, U., Ludwig, C., Zeuschner, D., and Gerke, V. (2003) The annexin 2/S100A10 complex controls the distribution of transferrin receptor-containing recycling endosomes, *Mol. Biol. Cell 14*, 4896−4908.
17. Hayes, M. J., Merrifield, C. J., Shao, D., Ayala-Sanmartin, J., Schorey, C. D., Levine, T. P., Proust, J., Curran, J., Bailly, M., and Moss, S. E. (2004) Annexin 2 binding to phosphatidylinositol 4,5-bisphosphate on endocytic vesicles is regulated by the stress response pathway, *J. Biol. Chem. 279*, 14157−14164.
18. Ross, M., Gerke, V., and Steinem, C. (2003) Membrane composition affects the reversibility of annexin A2t binding to solid supported membranes: A QCM study, *Biochemistry 42*, 3131−3141.
19. Gerke, V., and Weber, K. (1984) Identity of p36K phosphorylated upon Rous sarcoma virus transformation with a protein purified from brush borders; calcium-dependent binding to non-erythroid spectrin and F-actin, *EMBO J. 3*, 227−233.
20. Gerke, V., Creutz, C. E., and Moss, S. E. (2005) Annexins: Linking Ca^{2+} signalling to membrane dynamics, *Nat. Rev. Mol. Cell Biol. 6*, 449−461.
21. Kastl, K., Ross, M., Gerke, V., and Steinem, C. (2002) Kinetics and thermodynamics of annexin A1 binding to solid-supported membranes: A QCM study, *Biochemistry 41*, 10087−10094.
22. Ross, M., Steinem, C., Galla, H.-J., and Janshoff, A. (2001) Visualization of chemical and physical properties of calcium-induced domains in DPPC/DPPS Langmuir−Blodgett layers, *Langmuir 17*, 2437−2445.
23. Zeuschner, D., Stoorvogel, W., and Gerke, V. (2001) Association of annexin 2 with recycling endosomes requires either calcium- or cholesterol-stabilized membrane domains, *Eur. J. Cell Biol. 80*, 499−507.
24. Mukhopadhyay, S., and Cho, W. (1996) Interactions of annexin V with phospholipid monolayers, *Biochim. Biophys. Acta 1279*, 58−62.
25. Rosengarth, A., Wintergalen, A., Galla, H.-J., Hinz, H.-J., and Gerke, V. (1998) Ca^{2+}-independent interaction of annexin I with phospholipid monolayers, *FEBS Lett. 438*, 279−284.
26. Wu, F., Gericke, A., Flach, C. R., Mealy, T. R., Seaton, B. A., and Mendelsohn, R. (1998) Domain structure and molecular conformation in annexin V/1,2-dimyristoyl-*sn*-glycero-3-phosphate/Ca^{2+} aqueous monolayers: A Brewster angle microscopy/infrared reflection−absorption spectroscopy study, *Biophys. J. 74*, 3273−3281.
27. Pigault, C., Follenius-Wund, A., Schmutz, M., Freyssinet, J.-F., and Brisson, A. (1994) Formation of two-dimensional arrays of annexin V on phosphatidylserine-containing liposomes, *J. Mol. Biol. 236*, 199−208.
28. Reviakine, I., Bergsma-Schutter, W., Mazères-Dubut, C., Govorukhina, N., and Brisson, A. (2000) Surface topography of the p3 and the p6 annexin V crystal forms determined by atomic force microscopy, *J. Struct. Biol. 131*, 234−239.
29. Reviakine, I., Bergsma-Schutter, W., Morozov, A. N., and Brisson, A. (2001) Two-dimensional crystallization of annexin A5 on phospholipid bilayers and monolayers: A solid−solid phase transition between crystal forms, *Langmuir 17*, 1680−1686.
30. Mo, Y., Campos, B., Mealy, T. R., Commodore, L., Head, J. F., Dedman, J. R., and Seaton, B. A. (2003) Interfacial basic cluster in annexin V couples phospholipid binding and trimer formation on membrane surfaces, *J. Biol. Chem. 278*, 2437−2443.
31. Luecke, H. T., Chang. B. T., Mailliard, W. S., Schlaepfer, D. D., and Haigler, H. T. (1995) Crystal structure of the annexin XII hexamer and implications for bilayer insertion, *Nature 378*, 512−515.
32. Patel, D. R., Isas, J. M., Ladokhin, A. S., Jao, C. C., Kim, Y. E., Kirsch, T., Langen, R., and Haigler, H. T. (2005) The conserved core domains of annexins A1, A2, A5, and B12 can be divided into two groups with different Ca^{2+}-dependent membrane-binding properties, *Biochemistry 44*, 2833−2844.
33. Hinderliter, A., Almeida, P. F., Creutz, C. E., and Biltonen, R. L. (2001) Domain formation in a fluid mixed lipid bilayer modulated through binding of the C2 protein motif, *Biochemistry 40*, 4181−4191.
34. Janshoff, A., Ross, M., Gerke, V., and Steinem, C. (2001) Visualization of annexin I binding to calcium-induced phosphatidylserine domains, *ChemBioChem 2*, 587−590.

35. Richter, R. P., Maury, N., and Brisson, A. (2005) On the effect of the solid support on the interleaflet distribution of lipids in supported lipid bilayers, *Langmuir 21*, 299−304.
36. Dufrêne, Y. F., Boland, T., Schneider, J. W., Barger, W. R., and Lee, G. U. (1998) Characterization of the physical properties of model biomembranes at the nanometer scale with the atomic force microscope, *Faraday Discuss. 79*−*94*, 137−157.
37. Meyer, M., Hug, H. J., and Bennewitz, R. (2004) *Scanning Probe Microscopy*−*The Lab on a Tip*, Springer-Verlag, Berlin, Germany.
38. Menke, M., Ross, M., Gerke, V., and Steinem, C. (2004) The molecular arrangement of membrane-bound annexin A2-S100A10 tetramer as revealed by scanning force microscopy, *ChemBioChem 5*, 1003−1006.
39. Koppenol, S., Tsao, F. H., Yu, H., and Zografi, G. (1998) The interaction of lung annexin I with phospholipid monolayers at the air/water interface, *Biochim. Biophys. Acta 1369*, 221−232.
40. Eklund, K. K., Vuorinen, J., Mikkola, J., Virtanen, J. A., and Kinnunen, P. K. (1988) Ca^{2+}-induced lateral phase separation in phosphatidic acid/phosphatidylcholine monolayers as revealed by fluorescence microscopy, *Biochemistry 27*, 3433−3437.
41. Hui, S. W., Boni, L. T., Stewart, T. P., and Isac, T. (1983) Identification of phosphatidylserine and phosphatidylcholine in calcium-induced phase separated domains, *Biochemistry 22*, 3511−3516.
42. Bazzi, M. D., and Nelsestuen, G. L. (1991) Extensive segregation of acidic phospholipids in membranes induced by protein kinase C and related proteins, *Biochemistry 30*, 7961−7969.
43. Junker, M., and Creutz, C. E. (1993) Endonexin (annexin IV)-mediated lateral segregation of phosphatidylglycerol in phosphatidylglycerol/phosphatidylcholine membranes, *Biochemistry 32*, 9968−9974.
44. Lipowsky, R. (1993) Domain-induced budding of fluid membranes, *Biophys. J. 64*, 1133−1138.
45. Lipowsky, R. (1992) Budding of membranes induced by intramembrane domains, *J. Phys. II 2*, 1825−1840.

BI051585I